

Article

Digital Twin Modeling Method for Hierarchical Stiffened Plate Based on Transfer Learning

Ziyu Xu, Tianhe Gao, Zengcong Li, Qingjie Bi, Xiongwei Liu and Kuo Tian * 

Department of Engineering Mechanics, Key Laboratory of Digital Twin for Industrial Equipment, State Key Laboratory of Structural Analysis for Industrial Equipment, Dalian University of Technology, Dalian 116024, China

* Correspondence: tiankuo@dlut.edu.cn

Abstract: As the key load-bearing component of spacecraft, the strength evaluation of stiffened plate structures faces two challenges. On the one hand, the simulation results are sometimes inaccurate, due to the simplification of the true loading conditions and modeling details. On the other hand, data from the sensors cannot provide the full-field strength information of the structure, which may result in the misjudgment of the structural state. To this end, a digital twin modeling method of multi-source data fusion based on transfer learning is proposed in this paper. In transfer learning, simulation data and sensor data are utilized as the source dataset and the target dataset, respectively. First, a pre-trained deep neural network (DNN) model is established based on the source dataset. Then, the pre-trained DNN model is fine-tuned based on the target dataset using a lower learning rate and fewer training epochs. Finally, a digital twin model can be built, which is capable of visualizing the full-field strength information of the stiffened plate structure. To verify the effectiveness of the proposed method, an experimental study on a hierarchical stiffened plate is carried out. Compared with the traditional data fusion method, the results verify the high prediction accuracy and efficiency of the proposed method, demonstrating its potential for the strength health monitoring of spacecraft in orbit.



Citation: Xu, Z.; Gao, T.; Li, Z.; Bi, Q.; Liu, X.; Tian, K. Digital Twin Modeling Method for Hierarchical Stiffened Plate Based on Transfer Learning. *Aerospace* **2023**, *10*, 66. <https://doi.org/10.3390/aerospace10010066>

Academic Editor: Konstantinos Tserpes

Received: 2 December 2022

Revised: 28 December 2022

Accepted: 4 January 2023

Published: 9 January 2023



Copyright: © 2023 by the authors. Licensee MDPI, Basel, Switzerland. This article is an open access article distributed under the terms and conditions of the Creative Commons Attribution (CC BY) license (<https://creativecommons.org/licenses/by/4.0/>).

Keywords: digital twin; stiffened plate; transfer learning; multi-source data fusion; strength health monitor

1. Introduction

Stiffened plates are the key load-bearing component in manned spacecraft, space stations, and other aerospace structures [1,2]. When a spacecraft is in orbit, the stiffened plate structures of the spacecraft would suffer from unexpected events, such as crashes with meteoroids or orbital debris, as well as extremely harsh and complex working conditions [3]. By analyzing the strength condition (e.g., stress, strain) of the stiffened plates of the spacecraft, damage caused by strength failure, fatigue, and cracking can be detected.

The traditional health monitoring methods for stiffened plates of a spacecraft usually rely on ground-built physical accompanying flying systems, aiming to evaluate and simulate the performance of the true structure in orbit [4]. However, when the spacecraft suffers from unexpected events, such as crashes with meteoroids or orbital debris, the ground physical accompanying flight system cannot simulate the true working condition of the spacecraft in real-time. Meanwhile, the number of sensors placed in the spacecraft is usually insufficient, which makes it difficult to provide sufficient strength information. As a result, expert decision-making is seriously affected and the spacecraft structure and the safety of astronauts [5] may also be threatened.

As an integration of the physical entity and a virtual model, digital twin technology can provide a real-time, multi-dimension, multi-scale, and high-fidelity dynamic mapping of a physical entity [6,7]. Digital twin technology has been applied in structural health monitoring, operational maintenance, and life prediction, etc. In order to construct a high-precision digital twin model, it is essential to obtain an accurate simulation calculation.

Zarastvand et al. [8,9] devised an accurate simulation calculation method for stiffened plates, which provided simulation data for the construction of a digital twin model.

As the key to the digital twin, multi-source data fusion methods are important to ensure the prediction accuracy of the digital twin model. Liu et al. [10] built a variable fidelity model based on a generative adversarial network, which introduced a supervised loss strategy to improve the training efficiency, and verified the excellent prediction accuracy with fewer high-fidelity sample points for a steel plate structure case. Jin et al. [11] completed the fusion of variable fidelity data from different strain sensors based on a Gaussian regression model, aiming to monitor the strain of the whole structure with lower costs. Li et al. [12] proposed a digital twin model construction method based on multi-fidelity data fusion, illustrating the effectiveness of the method by engineering the case of an S-shaped variable cross-sectional stiffened curved shell. Tian et al. [13] provided a variable-fidelity surrogate model driven by transfer learning for stiffened shell buckling prediction problems. Milanoski et al. [14] completed the multi-level structural health monitoring of stiffened composite panels using digital twin technology. Song et al. [15] developed a variable fidelity model by considering simulation data and sensor data, and built a visual digital twin model of a truss case. Li et al. [16] proposed a multi-fidelity aerodynamic model based on a deep neural network, which could accurately predict the wing surface pressure with more simulation data and less sensor data. Overall, digital twin technology has demonstrated excellent application potential for aerospace structures.

Compared with the traditional strength health monitoring and maintenance methods of spacecraft, digital twin technology can combine the multi-source data of sensors and simulation. A digital twin model can effectively visualize the full-field strength variation of a structure and ensure the safety of the spacecraft's in-orbit operation and spacecraft personnel. However, how to build a digital twin model for spacecraft with digital twin technology remains a difficult and challenging task. To this end, the main purpose of this paper is to establish a novel multi-source data fusion method, aiming to build an accurate digital twin model for stiffened plates.

The rest of this paper is organized as follows: In Section 2, a digital twin modeling method for hierarchical stiffened plates, based on transfer learning, is described in detail. In Section 3, an example of an experimental study on a hierarchical stiffened plate is carried out and discussed. The conclusions of this work are drawn in Section 4.

2. Methodology

In this section, the proposed digital twin modeling method based on transfer learning for hierarchical stiffened plates is proposed. In Section 2.1, the traditional data fusion methods, including the hybrid bridge function method, the addition bridge function method, and the Co-Kriging method are introduced. In Section 2.2, the detailed steps of the proposed digital twin modeling method are described.

2.1. Traditional Multi-Fidelity Data Fusion Methods

In order to fuse multi-fidelity data (e.g., simulation data and sensor data), the bridge function method [17] and the Co-Kriging method [18] are widely applied in practical engineering [19].

The bridge function method mainly includes the addition bridge function [20], multiplication bridge function [21], and hybrid bridge function [22]. The output of the hybrid bridge function method can be calculated by

$$\hat{y}(x) = \rho \hat{y}_{LFM}(x) + \delta(x) \quad (1)$$

where $\hat{y}(x)$ denotes the response of the constructed digital twin, $\hat{y}_{LFM}(x)$ denotes a model built from structural simulation data, and the number of sample points in the model can

be controlled by sampling. $\hat{\delta}(x)$ denotes the error model built using sensors data and simulation data corresponding to the sensor coordinates, which can also be described by

$$\hat{\delta}(x) = y_{HFM}(x_{HFM}) - \rho \hat{y}_{LFM}(x_{HFM}) \quad (2)$$

where $y_{HFM}(x_{HFM})$ denotes the real measurement data of the structure by the sensors. The correction factor ρ is a constant that minimizes the error between $y_{HFM}(x_{HFM})$ and $\hat{y}_{LFM}(x_{HFM})$, whose value can be obtained by

$$\begin{aligned} & \text{find } \rho \\ & \min \sum_{i=1}^{n_{EXP}} [\rho \hat{y}_{LFM}(x_{HFM}^i) - y_{HFM}(x_{HFM}^i)]^2 \end{aligned} \quad (3)$$

where $y_{HFM}(x_{HFM}^i)$ denotes the real data of the structure measured by the sensor, and n_{EXP} denotes the total number of sensor measurement points.

To prove the validity of the proposed method, we also compared it with the addition bridge function method, the principle of which can be found in Ref. [23].

Co-Kriging is an extension of the traditional Kriging method [24], which assists in predicting the sensor data by introducing simulation data, to complete the construction of the structural digital twin model. The output of the digital twin model can be described by

$$\hat{y}(x) = \lambda_{HFM}^T y_{HFM} + \lambda_{LFM}^T y_{LFM} \quad (4)$$

where λ_{HFM}^T and λ_{LFM}^T are the weight coefficients associated with the sensors data and the simulation data after sampling, respectively. Their weight coefficients can be described using the following formula, which is related to the mean square error (MSE) and unbiased constraints.

$$MSE[\hat{y}_{HFM}(x)] = E[(\lambda_{HFM}^T y_{HFM} + \lambda_{LFM}^T y_{LFM} - y_{HFM})^2] \quad (5)$$

$$E[\lambda_{HFM}^T y_{HFM} + \lambda_{LFM}^T y_{LFM}] = E[y_{HFM}] \quad (6)$$

The minimum mean square error can be solved, to find the appropriate weight coefficients λ_{HFM}^T and λ_{LFM}^T . As the solution process is complicated, a more detailed derivation of the subsequent Co-Kriging method can be found in Ref. [24].

However, when facing complex problems such as the mechanical response analysis and prediction of the stiffened plates of spacecraft and as a result of the simple construction principle of the traditional hybrid bridge function method, this method cannot properly fuse multi-source data, leading to an unstable accuracy of digital twin models constructed using the hybrid bridge function method [25]. Due to the complex stiffened plate of a spacecraft, the finite element mesh division is detailed during the calculation, and more simulation data are generated after the completion of the calculation. In addition, the construction process of the Co-Kriging method is very complex, which leads to high construction costs and a low efficiency when building a digital twin model of the complex structure with the Co-Kriging method [26].

2.2. Digital Twin Modeling Method Based on Transfer Learning

The digital twin modeling of true structural strength conditions (e.g., stress and strain) is mainly based on the data fusion between sensors data and simulation data. Sensors data sample information is limited but can visualize the true mechanical response of a structure. The simulation data can provide the full-field strength information of the structure. However, the simulation results are sometimes inaccurate, due to the simplification of the loading conditions and modeling details. The main idea of a digital twin model is to make full use of these two kinds of data. In this section, transfer learning is utilized to build a digital twin model, aiming to predict the full-field strength information accurately.

First, the basic principle of DNN is briefly introduced. DNN is a neural network with input layer, hidden layer, and output layer, and the number of hidden layers is more than one. The training process of DNN is shown in Figure 1, which mainly includes three steps. In the first step, the training data is input into the DNN, and the forward calculation is carried out layer by layer, until reaching the output layer. In the second step, the predicted value of the current network output is compared with the real value, and the loss error is calculated using the loss function. In the final step, back propagation is carried out according to the chain rule, the gradient of the loss function on each layer is calculated, and the weight matrix is updated according to the weight gradient obtained in the reverse process. During several training iterations, the weight matrix is constantly updated to reduce the value of the loss function. At the same time, during the training process of the network, the dropout layer is used to discard the neurons in each layer from the network, according to a certain probability. This method can not only simplify the complex network model but also avoid overfitting.

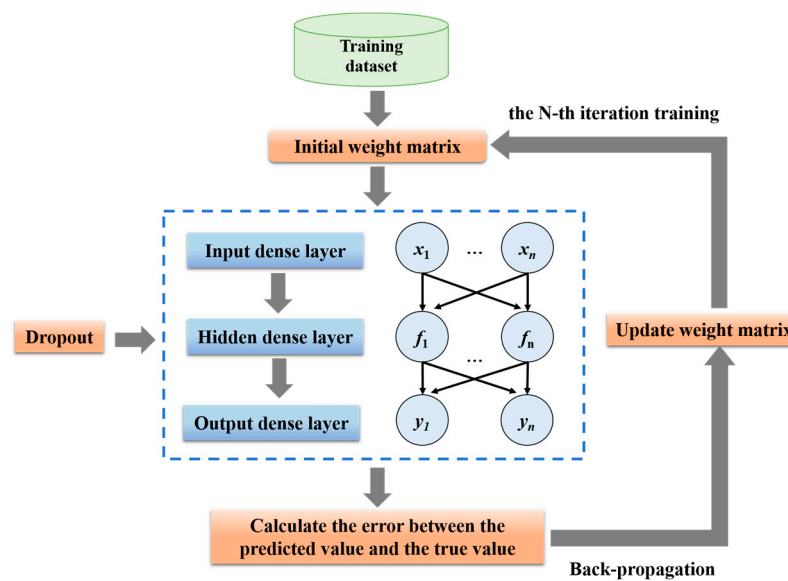


Figure 1. Schematic Diagram of the DNN Training Process.

In the DNN training process, the output h_j of hidden layer j can be described by

$$h_j = f(W_j h_{j-1} + b_j), \forall j \in \{1, 2, \dots, n\} \quad (7)$$

where h_{j-1} denotes the output of the formerly hidden layer and n is the total number of hidden layers. f denotes the activation function. Based on the activation function, the output of the current hidden layer can be used as the input of the next hidden layer. In this work, we use the ReLU function as the activation function [27]. W_j and b_j denote the weights and biases of the hidden layer, respectively. The loss function $L(\theta)$ [28] is established to obtain the value of the corresponding parameter $\theta = \{W_j, b_j\}_{j=1}^{n+1}$ in DNN, which can be described by

$$L(\theta) = \frac{1}{N} \sum_{i=1}^N E_i = \frac{1}{N} \sum_{i=1}^N (y_i^D - \hat{f}(x_i^D; \theta))^2 \quad (8)$$

where x_i^D and y_i^D denote the input and output of the training data, respectively. D denotes the dimension of the problem. N denotes the total amount of training data. $\hat{f}(x_i^D; \theta)$ denotes the predicted value of the DNN model after training under the parameter θ . The stochastic gradient descent with momentum (SGDM) algorithm [29] is used to minimize the Loss function $L(\theta)$. After the weights and biases of the hidden layers are determined, the training of the DNN is finished.

Transfer learning is an emerging machine learning method that has been extensively used in fields such as target detection and digital twin modeling. Transfer learning is applied for two tasks that are similar in certain ways, and the knowledge is transferred from one task to another task, which are different but similar [30]. In transfer learning, for the given source dataset D_s and source task T_s , target dataset D_t and target task T_t , there is either $D_s \neq D_t$ or $T_s \neq T_t$. Transfer learning can make full use of the information of D_s and T_s to effectively complete the training of T_t in D_t .

Hence, when constructing the digital twin model of the spacecraft structural strength conditions, utilizing the correlation between the sensor data and the simulation data, the knowledge migration from simulation data to sensor data is efficiently completed using simulation data and sensor data as the source data and target data, respectively, to build a digital twin model of the actual structural strength conditions (e.g., stress, strain). The process of digital twin modeling is described in Figure 2, which mainly involves the following five steps:

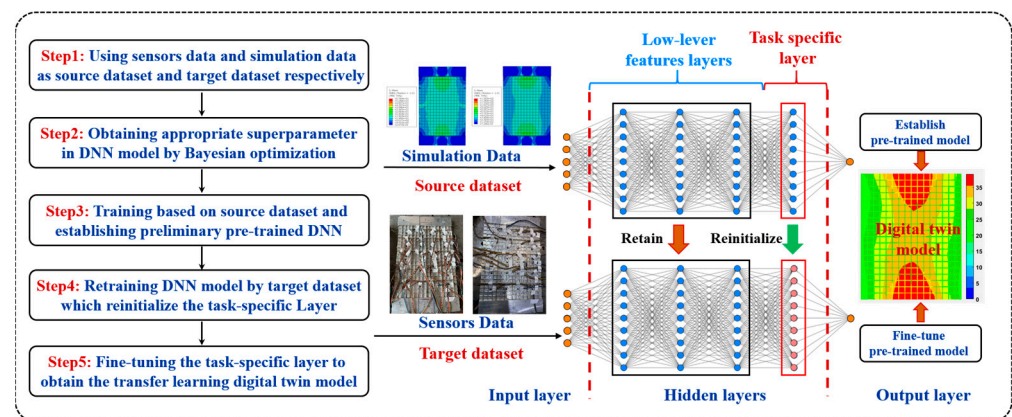


Figure 2. Digital twin modeling method based on transfer learning.

Step 1: The simulation data are sampled from the finite element analysis results of the structure using the Latin hypercube sampling (LHS) method. The sensor data are generated from the physical entity. The simulation data and the sensor data are used as the source dataset and target dataset in the transfer learning, respectively. It is noteworthy that all of the sensor data are utilized as the target data, since there is only a limited number of sensors placed on the structure.

Step 2: Suitable hyperparameters of the DNN model are obtained based on the Bayesian optimization (BO) method. In the optimization iteration, the simulation data and the sensor data are used as the training dataset and the validation dataset of the DNN model, respectively. The optimization objective is to minimize the mean square error (MSE) of the DNN model. In this work, there are five hyperparameters that need to be optimized using BO, including the learning rate lr_1 , the number of neurons in the first hidden layer N_1 , the number of neurons in the last hidden layer N_2 , the total number of hidden layers N_3 , and the dropout rate dr_1 .

Step 3: The pre-trained DNN model is obtained based on the source dataset with the hyperparameters obtained from the BO.

Step 4: In the DNN model, the early layers represent the low-level features learned from the simulation data. The last hidden layer represents the high-level feature layer, which is also called the task-specific layer or advanced feature layer. Hence, the early layers of the pre-trained model are frozen, and the advanced feature layer is reinitialized using sensor data, to reset the weights and biases of this layer.

Step 5: By fine-tuning the pre-trained DNN model with a smaller learning rate and fewer training steps, digital twin modeling of multi-source data fusion based on the transfer learning is completed.

Based on the above steps, a digital twin model can be built, which can then be used to visualize the full-field strength variation of the structure.

3. Experiment and Discussion

To verify the effectiveness of the proposed method, an example of digital twin modeling of a hierarchical stiffened plate is carried out in this section. The geometric model and simulation results of the hierarchical stiffened plate are introduced in Section 3.1. The detailed experiment process of the hierarchical stiffened plate in the laboratory environment is described in Section 3.2. The digital twin modeling process of a hierarchical stiffened plate is demonstrated in Section 3.3.

3.1. Introduction of the Simulation Results of the Hierarchical Stiffened Plate

As shown in Figure 3, the hierarchical stiffened plate is mainly composed of two clamping blocks and a stiffened shell. The lower clamping block acts as a fixed boundary. Axial pressure is imposed on the upper clamping block. The overall height and width of the stiffened plate are 660 mm and 400 mm, respectively. The size of the two clamping blocks is 15 mm × 80 mm × 400 mm, and the stiffened skin is 400 mm × 500 mm × 1.5 mm. The hierarchical stiffened plate is composed of major stiffeners (with larger stiffener size) and minor stiffeners (with smaller stiffener size). The number of minor stiffeners is 12, with a height of 5 mm and a thickness of 2 mm. The number of major stiffeners is 3, with a height of 10 mm and a thickness of 2 mm. These two types of stiffeners are staggered at equal distances along the width direction of the plate. In the direction of the plate width, the stiffeners are also divided into two types, and their heights are 10 mm and 5 mm, respectively. As the clamping blocks only partially touch the rigid fixtures of the test loading equipment, the boundary conditions are constrained by coupling the two faces in the clamping blocks after the actual loading position has been determined. The clamping height of the clamping block (loading area) is 65 mm, and the clamping height of the clamping block (boundary fixed area) is 70 mm, both clamping areas are located in the middle of the clamping block.

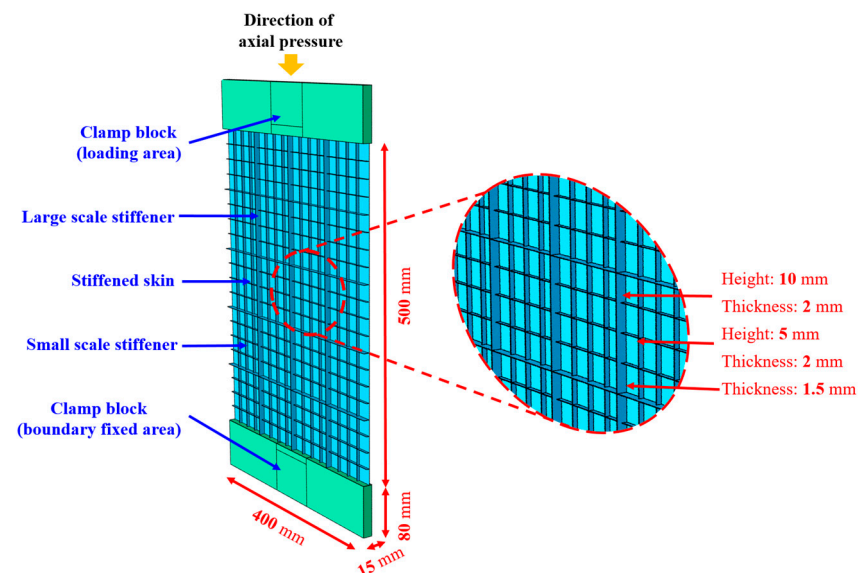


Figure 3. Geometric model of the hierarchical stiffened plate.

A geometric model of the hierarchical stiffened plate is constructed using the commercial software ABAQUS. The material of the hierarchical stiffened pane is 6061 T651 aluminum alloy, which has the following material properties: Elastic Modulus $E = 69.8$ GPa, Poisson's Ratio $\nu = 0.33$, Yield Stress $\sigma_s = 276$ MPa, Ultimate Stress $\sigma_b = 310$ MPa, Density $\rho = 2.7 \times 10^{-6}$ kg/mm³.

For the finite element model of the hierarchical stiffened plate, the S4R element is utilized for the stiffened shell, and the C3D8R element is used for the clamping blocks. Based on the mesh convergence analysis listed in Table 1, the element size is 1.8 mm. The number of elements in the stiffened shell is 93,296, and the total number of elements in the structure is 159,824. The computer configuration is an Intel Xeon Gold 6248R @ 3.00 GHz, 256 G RAM.

Table 1. Mises stress and computational cost with different numbers of elements of the hierarchical stiffened plate.

Element Seed Size/(mm)	Number of Elements	Mises Stress/(MPa)	CPU Time/s
7	8032	67.17	277.7
5	11,640	61.65	296.3
4	15,888	63.48	315.8
3.5	21,644	70.62	326.9
3	32,128	92.3	638.6
2.8	39,024	106.6	695.4
2.4	46,560	110.1	714.8
2.2	54,736	111.7	755.1
2	80,860	112.3	1061.5
1.8	93,296	114	1237.6
1.6	116,864	115.2	1784.2

Based on the established finite element model, a displacement load is applied to the loading area of the clamping block using the explicit dynamics method [31], to ensure that the axial pressure loads applied will not buckle the hierarchical stiffened plate structure, and the reaction force–displacement curve is shown in Figure 4. From the curve, it can be seen that the hierarchical stiffened plate buckled at around 43 kN under the axial pressure, and the displacement is 0.55 mm at this time.

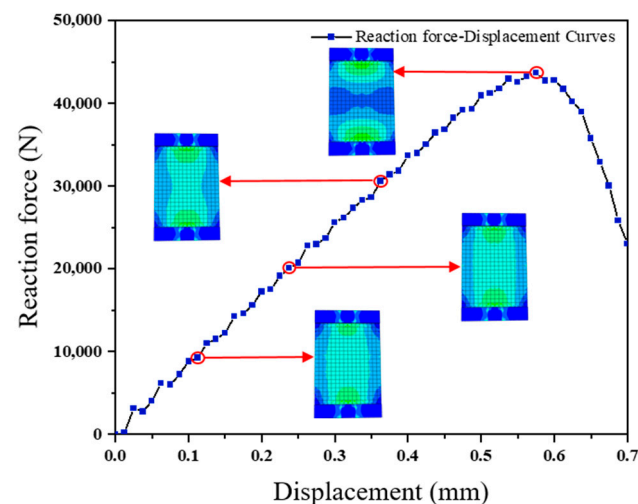


Figure 4. Reaction force–displacement curve of the hierarchical stiffened plate.

The simulation of the hierarchical stiffened plate is completed by 3.1. Then the Mises stress data of each node on the finite element model are extracted as the source dataset, in order to build a digital twin model of the hierarchical stiffened plate using the transfer learning method.

3.2. Experimental Process of the Hierarchical Stiffened Plate

In the experiment, a ground static test system (SHIMADZU EHF-UV 300 kN, made in Japan) is used to carry out the quasi-static axial pressure experiments. The specific

experimental setup is shown in Figure 5. The top and bottom of the hierarchical stiffened plate are the rigid fixtures. According to the simulation results, the final reaction force of the hierarchical stiffened plate is set as approximately 40% (about 18 kN) of the limit buckling load. In addition, the loading speed is set as 2 kN/min. The reaction force and displacement data are recorded by the control system.

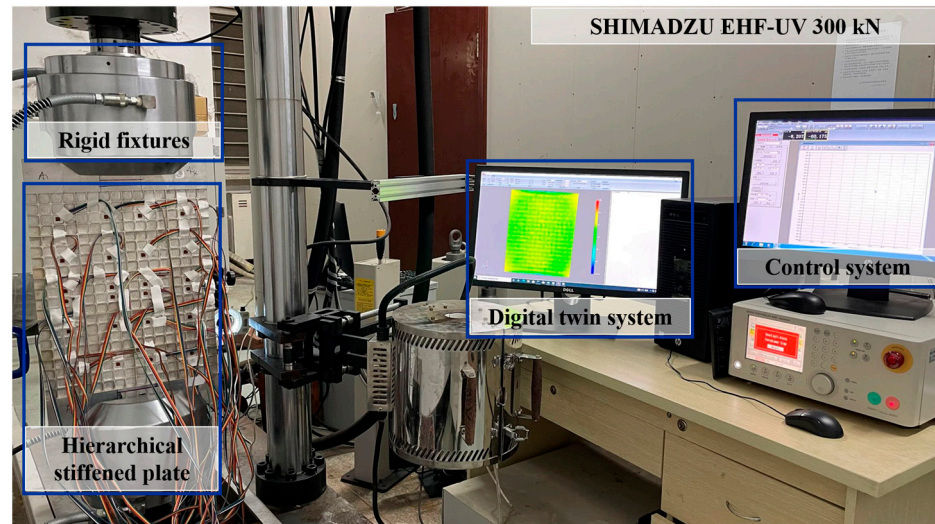


Figure 5. Static axial pressure digital twin experimental setup for the hierarchical stiffened plate.

As displayed in Figure 6, 24 right-angle strain rosettes are placed on the shell with 6 rows and 4 columns. The resistance of the deployed sensors is 121Ω , and the sensitivity factor is 2.12. They are also self-compensating and are connected to the strain-collection device via a three-wire connection, which is also called a quarter bridge, to eliminate the effect of the wire resistance on the data measurement. The collection device is Donghua Static Strain Collector 3816 N with 72 channels.

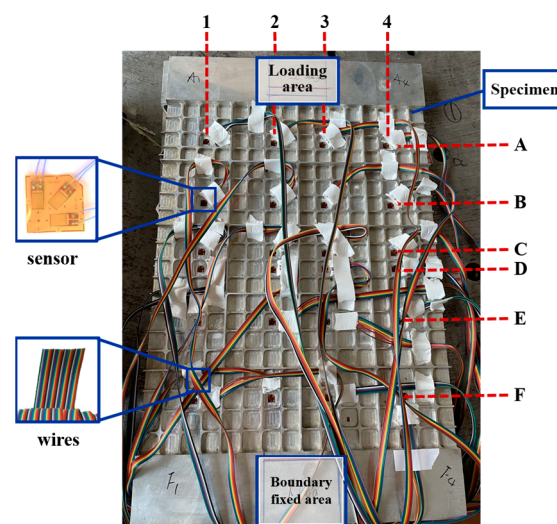


Figure 6. Layout of the sensors on the hierarchical stiffened plate.

The full measurement data for each sensor during the loading are obtained using a Donghua Static Strain Collector after the experiment has been completed. As a total of 24 strain rosettes are used in the experiment, there are 72 columns of strain data, varying with time. To ensure that the sensors is not destroyed during the experiment, each column of strain data should be checked. The strain data for all sensors with various loads are recorded according to the loading time. The location of each sensor is matched to the data

according to the correspondence of the sensor coordinates to the channels. To make it easier to calculate the Mises stress of the sensors, data from the three directions of the sensors are classified.

To obtain the Mises stress values, it is necessary to calculate the strain data from three channels. First, two principal stresses σ_1 and σ_2 can be calculated by

$$\left. \begin{matrix} \sigma_1 \\ \sigma_2 \end{matrix} \right\} = \frac{E}{1-\nu^2} \left[\frac{1+\nu}{2} (\varepsilon_0 + \varepsilon_{90}) \pm \frac{1+\nu}{\sqrt{2}} \sqrt{(\varepsilon_0 - \varepsilon_{45})^2 + (\varepsilon_{45} - \varepsilon_{90})^2} \right] \quad (9)$$

where ε_0 , ε_{45} , and ε_{90} denote the strains in each of the three directions measured by the right-angle strain rosette sensor, respectively. E and ν denote the elastic modulus and the Poisson's ratio of the structural material, respectively. Then, the Mises stress can be obtained by

$$\sigma = \sqrt{\frac{1}{2} [(\sigma_1 - \sigma_2)^2 + (\sigma_2 - \sigma_3)^2 + (\sigma_3 - \sigma_1)^2]} \quad (10)$$

where σ_3 denotes the value is 0 for the principal stress, as the strain rosette sensor is a planar stress state. Based on Equations (9) and (10), the Mises stress data for the hierarchical stiffened plate at 18 kN operating conditions can be obtained, which is listed in Table 2.

Table 2. Calculation of Mises stress in the hierarchical stiffened plate (MPa).

Sensor's Location	1	2	3	4
A	21.33	31.99	31.86	23.00
B	20.37	26.50	26.34	20.42
C	19.58	25.01	25.35	19.68
D	19.13	24.78	24.93	20.09
E	17.89	26.31	27.04	17.89
F	18.59	31.81	32.00	20.64

As can be seen from Table 2, the stress values for the sensors are symmetrical. However, the data for sensor number A4 is slightly larger than that of sensor A1, and the same occurs between F4 and F1, which indicates a slight eccentricity of loading within the permissible limits of the test, meaning that the rigid fixture is not exactly in the middle of the clamping block.

The static axial pressure test of the hierarchical stiffened plate is detailed in Section 3.2. The Mises stress data of the sensors are calculated as the target dataset. Combined with the simulation data, a digital twin model of the hierarchical stiffened plate could be constructed based on the transfer learning multi-source data fusion method.

3.3. Comparison between the Proposed Method and the Traditional Methods

Based on the simulation data and experimental data obtained in Sections 3.1 and 3.2, data fusion models are established in this section. In this study, the leave-one-out validation approach is employed to evaluate the accuracy of the traditional methods and the proposed method. Specifically, if there are N sensor samples, the former $N-1$ sensor samples are used as the training set to build the digital twin model, and the last sensor sample is used as the testing set. Each sample point is going to be used as the testing set once, and N times of the calculation are needed to obtain the accuracy of the digital twin model, which can be expressed as

$$\text{Acc} = \frac{\sum_{i=1}^N \left(1 - \frac{|y_i^{\text{HFM}} - y_i^{\text{DT}}|}{|y_i^{\text{HFM}}|} \right)}{N} \quad (11)$$

where N denotes the number of sensors, and y_i^{HFM} and y_i^{DT} denote the true value of that sensor data and the predicted value by the digital twin model, respectively. The closer y approaches to 1, the more accurate the model is.

A digital twin model for the hierarchical stiffened plate with multi-source data fusion is constructed based on the method proposed in Section 2.2.

First, 3000 points are sampled using LHS from the simulation data of the hierarchical stiffened plate at 18 kN, which is used as the source dataset, also called a low-fidelity model (LFM). The sensor data are used as the target dataset, also called a high-fidelity model (HFM). Then, the hyper-parameters of the DNN model could be determined based on the BO: the total number of hidden layers is 6, the number of neurons in the first hidden layer is 100, the number of neurons in the last hidden layer is 50, the dropout rate is 0.4, and the learning rate is 0.0015. Next, a pre-trained DNN model has been built based on the source dataset, where the number of iteration steps of the SGDM algorithm is 1000. Afterward, the low-level feature layer of the DNN is frozen. The weights and biases of the high-level feature layers are reinitialized. Finally, the DNN model is fine-tuned based on the target dataset, and a digital twin model of the hierarchical stiffened plate is constructed.

To make a comparison with the traditional data fusion methods, the hybrid bridge function method [22], the addition bridge function method [23], and the Co-Kriging method [24] are used to calculate the accuracy using the same experimental and simulation data. To reflect the variety in the results, besides the construction of the digital twin model of the hierarchical stiffened plate at 18 kN, the construction of the digital twin models for the hierarchical stiffened plate at 15 kN and 10 kN are also completed using the various digital twin data fusion methods mentioned above. The prediction accuracy and the computation cost of the various digital twin data fusion models are displayed in Table 3.

Table 3. The prediction accuracy and computational cost of the various data fusion models for the hierarchical stiffened plate.

		Co-Kriging Method [24]		Hybrid BridgeFunction Method [22]		Addition Bridge Function Method [23]		Proposed Method	
		Acc	CPU time/s	Acc	CPU time/s	Acc	CPU time/s	Acc	CPU time/s
18 kN	1500 LFM + 24 HFM	0.9543	350.59	0.6931	0.36	0.5083	0.13	0.9546	24.01
	3000 LFM + 24 HFM	0.9394	4861.22	0.6697	0.73	0.4729	0.46	0.9532	40.46
	4800 LFM + 24 HFM	-	-	0.7412	2.64	0.4526	1.32	0.9531	64.33
15 kN	1500 LFM + 24 HFM	0.9471	339.64	0.6187	0.34	0.5250	0.14	0.9575	26.06
	3000 LFM + 24 HFM	0.9523	4902.6	0.6925	0.81	0.5422	0.47	0.9617	38.92
	4800 LFM + 24 HFM	-	-	0.6572	2.48	0.4507	1.37	0.9614	68.58
10 kN	1500 LFM + 24 HFM	0.9539	356.27	0.6280	0.32	0.4922	0.13	0.9588	25.29
	3000 LFM + 24 HFM	0.9559	4684.75	0.6928	0.69	0.4689	0.47	0.9592	42.07
	4800 LFM + 24 HFM	-	-	0.6618	2.59	0.4201	1.34	0.9580	65.91

As can be seen from Table 3, when the sample dataset is made up of 24 sensors data and 3000 simulation data, the computational cost of the proposed method is only 0.832% of the Co-Kriging method, while the prediction accuracy is slightly better than that of the Co-Kriging method, which verifies the efficiency advantage of the proposed method. In order to further verify the robustness of the proposed method, the number of simulation data at various loads is sampled into two groups of 1500 and 4800, respectively. As shown in Table 3 and Figure 7, in the digital twin model constructed for the hierarchical stiffened plate of 18 kN, the proposed method have the best prediction accuracy among the various combinations of simulation data and sensor data. The prediction accuracy of the digital twin model built using the proposed method is 28.35%, 48.03%, and 1.38% higher than

that of the hybrid bridge function method, the addition bridge function method, and Co-Kriging method, respectively. With the group of 24 sensor data and 3000 simulation data, the high prediction accuracy of the proposed method is illustrated. The results of the digital twin model under other loads also follow the same trend. It is worth noting that the time required for the digital twin model to complete leave-one-out validation with 3000 simulation data increases from 2 h to more than 1 day compares to 1500 simulation data, due to the complexity of the Co-Kriging method. Hence, the calculation data of the Co-Kriging method for 4800 simulation data are not shown.

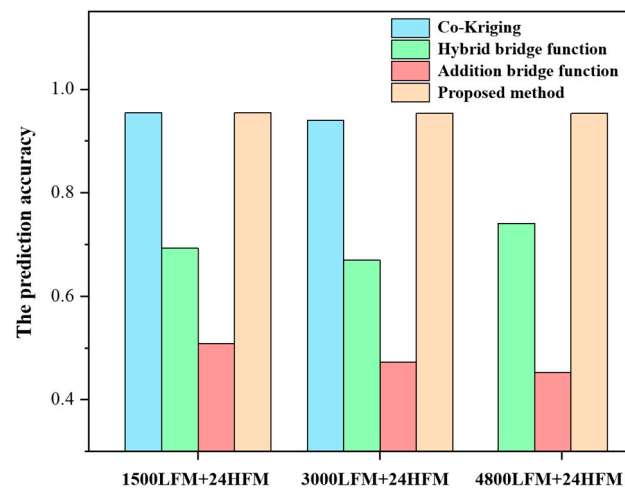


Figure 7. The prediction accuracy of the various digital twin models for the hierarchical stiffened plate at 18 kN.

The Mises stress field diagrams for the digital twin models of the hierarchical stiffened plate constructed using various methods at 18 kN are shown in Figure 8. As can be seen from Figure 8, the cloud map of the digital twin model constructed using the proposed method has a clearer and smoother display. Meanwhile, it can be seen from the Mises stress field diagrams of the proposed method that the test loading is slightly eccentric, which also consistent with the results obtained during the processing of the experimental data. The stress prediction amplitude from each model shows that the danger area of stress is located at the connections between the skin and the clamping blocks. When comparing with Table 2, it can be seen that the stress amplitude and stress distribution of digital twin model constructed using the proposed method are more consistent with the sensor data, which again demonstrates the high prediction accuracy and robustness of the proposed method. Overall, the proposed digital twin modeling method demonstrates its outstanding accuracy and applicability during the experimental study of hierarchical stiffened plate.

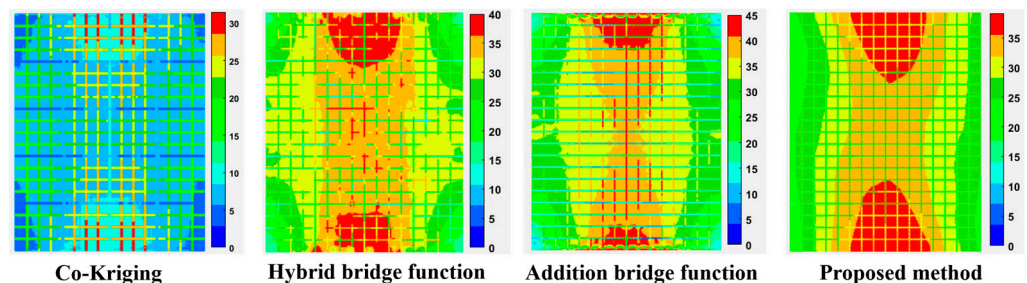


Figure 8. Mises stress field diagrams of various digital twin models for the hierarchical stiffened plate at 18 kN.

4. Conclusions

To obtain the full-field strength variation of a structure, a digital twin modeling method based on transfer learning for multi-source data fusion is proposed. First, the

simulation data is sampled by LHS. Then, a pre-trained DNN model is obtained based on the simulation data, and suitable hyperparameters for the DNN model are obtained by BO. Finally, the initial layers of the pre-trained model are frozen, and the digital twin mode has been established by fine-tuning the sensor data. To verify the effectiveness of the proposed method, an experimental study is carried out using static axial pressure testing of the hierarchical stiffened plate. The results show that the proposed method required only 0.832% of the computational cost of the Co-Kriging method with the same prediction accuracy, which verify the efficiency of the proposed method. Meanwhile, the leave-one-out validation accuracy of the digital twin model constructed using the proposed method improves by 28.35%, 48.03%, and 1.38% over the hybrid bridge function method, the addition bridge function method, and the Co-Kriging method, respectively, illustrating its high prediction accuracy. Overall, the proposed method could be applied for the strength health monitoring of spacecraft stiffener structures and has the potential to ensure spacecraft operation in orbit and crew safety.

In a future study, a multi-scale strategy could be applied in digital twin model construction for more complex stiffened plate structures, with the aim of improving the accuracy and reliability of the method for strength health monitoring.

Author Contributions: Conceptualization, Z.X. and Z.L.; methodology, Z.X., Z.L., T.G., and K.T.; validation, Z.X., Z.L., T.G., Q.B., and X.L.; formal analysis, Z.X.; investigation, T.G. and Z.L.; data curation, Z.X., T.G., Q.B., and X.L.; writing—original draft preparation, Z.X.; writing—review and editing, Z.X., Z.L., and K.T.; supervision, K.T.; funding acquisition, K.T. All authors have read and agreed to the published version of the manuscript.

Funding: National Key Research and Development Program project of China (2022YFB3404700); National Natural Science Foundation of China (11902065); Fundamental Research Funds for the Central Universities (DUT21RC(3)013).

Institutional Review Board Statement: Not applicable.

Informed Consent Statement: Informed consent was obtained from all subjects involved in the study.

Data Availability Statement: Not applicable.

Conflicts of Interest: The authors declare no conflict of interest.

Abbreviations

The following abbreviations are used in this manuscript:

BO	Bayesian Optimization
DNN	Deep Neural Network
LHS	Latin Hypercube Sampling
MSE	Mean Square Error
SGDM	Stochastic Gradient Descent with Momentum
LFM	low-fidelity model
HFM	high-fidelity model

References

1. Tian, K.; Lai, P.; Sun, Y.; Sun, W.; Cheng, Z.; Wang, B. Efficient buckling analysis and optimization method for rotationally periodic stiffened shells accelerated by Bloch wave method. *Eng. Struct.* **2023**, *276*, 115395. [[CrossRef](#)]
2. Wang, D.; Hui, J.; Cao, W.; Yang, Y.; Wan, Y.; Zuo, H.; Zhang, B. The influence of geometric imperfections on post-buckling behavior and free vibrations of a fiber-reinforced composite laminated plate under thermal loading. *Compos. Struct.* **2022**, *306*, 116568. [[CrossRef](#)]
3. Ye, Y.; Yang, Q.; Yang, F.; Huo, Y.; Meng, S. Digital twin for the structural health management of reusable spacecraft: A case study. *Eng. Fract. Mech.* **2020**, *234*, 107076. [[CrossRef](#)]
4. Schleich, B.; Anwer, N.; Mathieu, L.; Wartzack, S. Shaping the digital twin for design and production engineering. *CIRP Ann.* **2017**, *66*, 141–144. [[CrossRef](#)]
5. Shi, J.-X.; Nagano, T.; Shimoda, M. Fundamental frequency maximization of orthotropic shells using a free-form optimization method. *Compos. Struct.* **2017**, *170*, 135–145. [[CrossRef](#)]

6. Liu, M.; Fang, S.; Dong, H.; Xu, C. Review of digital twin about concepts, technologies, and industrial applications. *J. Manuf. Syst.* **2021**, *58*, 346–361. [[CrossRef](#)]
7. Jones, D.; Snider, C.; Nassehi, A.; Yon, J.; Hicks, B. Characterising the Digital Twin: A systematic literature review. *CIRP J. Manuf. Sci. Technol.* **2020**, *29*, 36–52. [[CrossRef](#)]
8. Zarastvand, M.R.; Ghassabi, M.; Talebitooti, R. Prediction of acoustic wave transmission features of the multilayered plate constructions: A review. *J. Sandw. Struct. Mater.* **2022**, *24*, 218–293. [[CrossRef](#)]
9. Zarastvand, M.R.; Ghassabi, M.; Talebitooti, R. A Review Approach for Sound Propagation Prediction of Plate Constructions. *Arch. Comput. Methods Eng.* **2021**, *28*, 2817–2843. [[CrossRef](#)]
10. Liu, L.; Song, X.; Zhang, C.; Tao, D. GAN-MDF: An Enabling Method for Multi-fidelity Data Fusion. *IEEE Internet Things J.* **2022**, *9*, 13405–13415. [[CrossRef](#)]
11. Jin, S.-S.; Kim, S.T.; Park, Y.-H. Combining point and distributed strain sensor for complementary data-fusion: A multi-fidelity approach. *Mech. Syst. Signal Process.* **2021**, *157*, 107725. [[CrossRef](#)]
12. Li, Z.; Zhang, S.; Li, H.; Tian, K.; Cheng, Z.; Chen, Y.; Wang, B. On-line transfer learning for multi-fidelity data fusion with ensemble of deep neural networks. *Adv. Eng. Inform.* **2022**, *53*, 101689. [[CrossRef](#)]
13. Tian, K.; Li, Z.; Zhang, J.; Huang, L.; Wang, B. Transfer learning based variable-fidelity surrogate model for shell buckling prediction. *Compos. Struct.* **2021**, *273*, 114285. [[CrossRef](#)]
14. Milanoski, D.; Galanopoulos, G.; Zarouchas, D.; Loutas, T. Multi-level damage diagnosis on stiffened composite panels based on a damage-uninformative digital twin. *Struct. Health Monit.* **2022**. [[CrossRef](#)]
15. Wang, S.; Lai, X.; He, X.; Qiu, Y.; Song, X. Building a Trustworthy Product-Level Shape-Performance Integrated Digital Twin with Multifidelity Surrogate Model. *J. Mech. Des.* **2022**, *144*, 031703. [[CrossRef](#)]
16. Li, K.; Kou, J.; Zhang, W. Deep Learning for Multifidelity Aerodynamic Distribution Modeling from Experimental and Simulation Data. *AIAA J.* **2022**, *60*, 4413–4427. [[CrossRef](#)]
17. Gano, S.E.; Renaud, J.E.; Sanders, B. Hybrid Variable Fidelity Optimization by Using a Kriging-Based Scaling Function. *AIAA J.* **2005**, *43*, 2422–2433. [[CrossRef](#)]
18. Le Gratiet, L.; Garnier, J. Recursive Co-Kriging Model for Design of Computer Experiments with Multiple Levels of Fidelity. *Int. J. Uncertain. Quantif.* **2014**, *4*, 365–386. [[CrossRef](#)]
19. Fernández-Godino, M.G.; Park, C.; Kim, N.H.; Haftka, R.T. Review of Multi-fidelity Models. *arXiv* **2016**, arXiv:160907196. [[CrossRef](#)]
20. Choi, S.; Alonso, J.J.; Kroo, I.M. Two-Level Multifidelity Design Optimization Studies for Supersonic Jets. *J. Aircr.* **2009**, *46*, 776–790. [[CrossRef](#)]
21. Haftka, R.T. Combining global and local approximations. *AIAA J.* **1991**, *29*, 1523–1525. [[CrossRef](#)]
22. Fernández-Godino, M.G.; Park, C.; Kim, N.H.; Haftka, R.T. Issues in Deciding Whether to Use Multifidelity Surrogates. *AIAA J.* **2019**, *57*, 2039–2054. [[CrossRef](#)]
23. Tian, K.; Li, Z.; Huang, L.; Du, K.; Jiang, L.; Wang, B. Enhanced variable-fidelity surrogate-based optimization framework by Gaussian process regression and fuzzy clustering. *Comput. Methods Appl. Mech. Eng.* **2020**, *366*, 113045. [[CrossRef](#)]
24. Han, Z.H.; Zimmermann, R.; Goretz, S. A New Cokriging Method for Variable-Fidelity Surrogate Modeling of Aerodynamic Data. In Proceedings of the 48th AIAA Aerospace Sciences Meeting Including the New Horizons Forum and Aerospace Exposition, Orlando, FL, USA, 4–7 January 2010.
25. Tian, K.; Li, Z.; Ma, X.; Zhao, H.; Zhang, J.; Wang, B. Toward the robust establishment of variable-fidelity surrogate models for hierarchical stiffened shells by two-step adaptive updating approach. *Struct. Multidiscip. Optim.* **2020**, *61*, 1515–1528. [[CrossRef](#)]
26. Han, Z.-H.; Görtz, S.; Zimmermann, R. Improving variable-fidelity surrogate modeling via gradient-enhanced kriging and a generalized hybrid bridge function. *Aerosp. Sci. Technol.* **2013**, *25*, 177–189. [[CrossRef](#)]
27. Eckle, K.; Schmidt-Hieber, J. A comparison of deep networks with ReLU activation function and linear spline-type methods. *Neural Netw.* **2019**, *110*, 232–242. [[CrossRef](#)]
28. Zhuang, F.; Qi, Z.; Duan, K.; Xi, D.; Zhu, Y.; Zhu, H.; Xiong, H.; He, Q. A Comprehensive Survey on Transfer Learning. *Proc. IEEE* **2020**, *109*, 43–76. [[CrossRef](#)]
29. Marei, M.; El Zaatari, S.; Li, W. Transfer learning enabled convolutional neural networks for estimating health state of cutting tools. *Robot. Comput. Manuf.* **2021**, *71*, 102145. [[CrossRef](#)]
30. Pan, S.J.; Yang, Q. A Survey on Transfer Learning. *IEEE Trans. Knowl. Data Eng.* **2009**, *22*, 1345–1359. [[CrossRef](#)]
31. Zhang, Z.; Ding, W.; Ma, H. Local stress analysis of a defective rolling bearing using an explicit dynamic method. *Adv. Mech. Eng.* **2016**, *8*, 1687814016679909. [[CrossRef](#)]

Disclaimer/Publisher’s Note: The statements, opinions and data contained in all publications are solely those of the individual author(s) and contributor(s) and not of MDPI and/or the editor(s). MDPI and/or the editor(s) disclaim responsibility for any injury to people or property resulting from any ideas, methods, instructions or products referred to in the content.